Quantifying Algal Biomass in Lake Rotorua: Laboratory-Based Chlorophyll-*a* Analysis Across Space and Time

For

STEMX573

A report prepared by

Kendall Williams

Supervised by Whitney Woelmer & Deniz Özkundakci

THE UNIVERSITY OF WAIKATO
Te Whare Wānanga o Waikato

2026

Highlights

- Nearshore algal blooms were episodic and spatially heterogeneous, not monotonic.
- Bloom exceedances (≥10 μg L^{-1} chl-*a*) were temporally clustered with lake-wide intensification in Weeks 2 and 6, with hotspots at inflow sites (e.g., Awahou).
- Wind exposure and shoreline morphology influenced bloom accumulation, favouring sheltered sites under calm conditions.
- The hand-held FluoroQuik sensor showed a significant but moderate global relationship with laboratory chl-*a* (R^2 = 0.30).
- Sensor performance was concentration-dependent and site-specific, reliably detecting elevated biomass under bloom conditions but showing low sensitivity at low chl-*a* (<10 μg L^{-1}).

Abstract

Freshwater algal blooms are an increasing global concern, particularly in eutrophic lakes where nutrient enrichment and climatic drivers promote episodic cyanobacterial proliferation. Lake Rotorua (New Zealand) is a shallow, polymictic, eutrophic lake that experiences recurrent nearshore blooms with ecological, cultural, and recreational implications. This study aimed to (1) quantify spatial and temporal variability in shoreline algal biomass using laboratory-based chlorophyll-*a* (chl-*a*) analysis, and (2) validate a hand-held fluorescence sensor (FluoroQuik) against laboratory measurements to assess its suitability for rapid operational monitoring. Surface water samples were collected weekly from nine shoreline sites over six weeks (November 2025–January 2026). Chlorophyll-*a* was extracted using buffered acetone and quantified fluorometrically following acidification correction. Sensor measurements were recorded concurrently. Bloom conditions were defined as chl-*a* ≥ 10 µg L^{-1} (NPS-FM Band A maximum threshold). Laboratory chl-*a* revealed highly heterogeneous, episodic bloom dynamics rather than monotonic seasonal trends. Distinct lake-wide pulses occurred in Weeks 2 and 6, while extreme site-specific events were observed at inflow-associated locations, particularly Awahou (Tarimano) (maximum 38.75 µg L^{-1}). Wind exposure influenced nearshore accumulation, with sheltered sites exhibiting higher biomass under calm conditions and exposed sites showing greater variability. Bloom exceedances were temporally clustered and spatially uneven, emphasising the importance of high-frequency, multi-site monitoring. FluoroQuik fluorescence showed a significant but moderate global relationship with laboratory chl-*a* (R^2 = 0.30, p < 0.001). Sensor performance was concentration-dependent: no relationship was observed below 10 µg L^{-1}, whereas a weak but significant relationship occurred under bloom conditions (R^2 = 0.18, p = 0.04). Site-specific variability further highlighted spatial limitations. Overall, nearshore bloom dynamics in Lake Rotorua are disturbance-driven and

spatially structured. Hand-held fluorescence sensors provide useful, rapid detection of elevated biomass but require site-specific validation before integration into management and forecasting frameworks.

Keywords

Lake Rotorua; Algal Blooms; Chlorophyll-*a*; Nearshore Monitoring; Fluorescence sensor; FluoroQuik; Laboratory Analysis; Polymictic Lake; Eutrophication; Cyanobacteria

Introduction

Lakes are bodies of water in deep depressions along the Earth's surface, formed by geological processes such as glaciers, landslides, wind, rivers, and anthropogenic interference (Burns *et al.*, 1999). Covering ~1.8% of the earth's land area, lakes act as deep depositories and reservoirs for ecological, cultural, recreational, and economic resources (Wu *et al.*, 2023). Lake health is influenced by both natural processes (e.g., eutrophication, stratification) and anthropogenic pressures (such as agricultural catchment inputs) (Burns, 1991). They are dynamic, supporting a wide range of aquatic life (e.g., bacteria, plankton, plants, insects and fish) and influencing surrounding terrestrial ecosystems (Britton *et al.*, 1975).

Freshwater algal blooms are a growing global environmental concern, with increasing frequency, duration, and intensity reported across lakes and reservoirs worldwide (O'Neil *et al.*, 2012; Paerl *et al.*, 2018; Kraft *et al.*, 2025). These blooms are most commonly driven by eutrophication, a process characterised by excess nutrient loading–particularly phosphorus and nitrogen–combined with favourable climatic conditions such as elevated temperatures, high irradiance, and altered mixing regimes (Burns, 1991; Moss, 1998; Hamilton, 2003; Ho *et al.*, 2019). While eutrophication can occur naturally over geological timescales, accelerated eutrophication associated with human activities (e.g., intensive agricultural or pastoral use nearby) has become the dominant driver for more frequent algal bloom events and deoxygenation of bottom waters, leading to overall ecological decline and indications of poor water quality (Moss, 1998; Burns *et al.*, 1999).

Cyanobacteria frequently dominate bloom events in eutrophic and polymictic (experiencing shallow, diurnal stratification during the day due to solar heating, then returning to a fully mixed isothermal state at night) lakes and pose particular concerns due to their ability to produce cyanotoxins that threaten ecosystem functioning, drinking water supplies, and human and animal health (Codd *et al.*, 2005; Hodges *et al.*, 2018). Exposure to cyanotoxins

may cause dermatological, neurological, hepatic, respiratory, and gastrointestinal effects through contact or ingestion of contaminated water, resulting in public health advisories, recreational closures, and substantial socio-economic impacts (Cotterill *et al.*, 2019). Consequently, effective monitoring of algal biomass and bloom development is a central component of lake management strategies worldwide to maintain their integrity.

Chlorophyll-*a* as a Proxy for Algal Biomass

Chlorophyll-*a* (chl-*a*) concentration (μg L^{-1}) is widely used as a standard proxy for phytoplankton biomass and bloom intensity in freshwater systems (Thomson-Laing *et al.*, 2020). As the primary photosynthetic pigment common to most algal taxa, chl-*a* provides a quantitative, integrative measure of algal abundance that is comparable across sites, seasons, and monitoring programmes (Hötzel & Croome, 1999; Roesler *et al.*, 2017). Chlorophyll-*a* is a core component of widely adopted water quality indices, including the Trophic Level Index (TLI), which integrates chl-*a* with total nitrogen, total phosphorus, and Secchi depth to assess lake trophic status (i.e., water quality) in Aotearoa New Zealand (Burns *et al.*, 2005; Wu *et al.*, 2023).

Laboratory-based chl-*a* analysis using extractive fluorometry or spectrophotometry remains the gold-standard method for estimating algal biomass due to its accuracy and robustness (Hötzel & Croome, 1999; Hodges *et al.*, 2018). However, these methods are time- and resource-intensive, require specialised equipment and expertise, and involve delays between sample collection and result availability, limiting their utility for rapid decision-making during bloom events (Hodges *et al.*, 2018; Thomson-Laing *et al.*, 2020; Hamdhani *et al.*, 2021).

Advances in Fluorescence-based Sensing and the Need for Validation

To address these limitations, fluorescence-based sensors have been increasingly developed and deployed to provide rapid, cost-effective proxy measurements of algal biomass (Nelson *et al.*, 2009; Roesler *et al.*, 2017). Hand-held fluorometers (e.g., the FluoroQuik) offer particular advantages for operational monitoring, including portability, low cost, minimal technical expertise requirements, and real-time data acquisition (Hodges *et al.*, 2018; Hamdhani *et al.*, 2021). These tools are especially valuable in monitoring programmes involving multiple sites, nearshore sampling, or responsive sampling during bloom events at unmonitored locations (Cotterill *et al.*, 2019).

Despite their promise, fluorescence sensors (more so probes than hand-held) can be influenced by environmental factors such as ambient light, water temperature, and interference from non-target algal groups, leading to variability in the relationship between fluorescence signals and extracted chl-*a* concentrations (Roesler *et al.*, 2017; Hodges *et al.*, 2018). Consequently, sensor outputs require careful validation against laboratory measurements, ideally across a range of spatial, temporal, and ecological conditions, before they can be reliably integrated into monitoring and management frameworks (Hodges *et al.*, 2018; Thomson-Laing *et al.*, 2020).

Importance of Inshore Sampling

Monitoring efforts in many lakes have traditionally focused on offshore or pelagic sites, yet nearshore zones often experience the most severe and socially relevant impacts of algal blooms (Kraft *et al.*, 2025). Wind-driven surface transport, reduced vertical mixing, and shoreline morphology frequently result in the accumulation of phytoplankton biomass and surface scums along lake margins, even when offshore concentrations remain comparatively low (Deng *et al.*, 2016; Wu *et al.*, 2023). Nearshore zones are also more directly influenced by

nutrient inputs from inflowing streams, groundwater seepage, stormwater discharge, and adjacent urban pastoral land use (Moss, 1998; Hamilton, 2003; Wu *et al.,* 2023).

In polymictic lakes, intermittent stratification events lasting from hours to weeks can further exacerbate nearshore bloom development by promoting internal nutrient loading from bottom sediments during periods of deoxygenation (Rutherford *et al.,* 1996; Hamilton, 2003). Especially in nearshore areas of shallow lakes, wind-driven resuspension of sediments can also reintroduce nutrients into the water column. These processes highlight the importance of targeted shoreline monitoring to capture fine-scale spatial heterogeneity, provide early detection of bloom formation, and assess exposure risks most relevant to recreational users and local communities (Cotterill *et al.,* 2019; Kraft *et al.,* 2025).

Lake Rotorua as a Case Study

Lake Rotorua is a shallow (mean depth ~11 m; maximum depth ~45 m), polymictic, eutrophic lake within the Te Arawa Lakes system in the central North Island of Aotearoa, New Zealand (Hamilton, 2003; Pearson *et al.,* 2010). Formed approx. 200,000 years ago, within the Taupō Volcanic Zone, the lake is influenced by geothermally heated surface and subsurface inflows that contribute phosphorus and trace metals to the system (Pearson *et al.,* 2010; Wu *et al.,* 2023). The lake has a large catchment-to-volume ratio and has experienced extensive land-use change since European settlement, including urban expansion and conversion of native forest to pasture, resulting in elevated nutrient loads from both point (e.g., sewage piping/outflows) and diffuse (e.g., agricultural run-off) sources (McColl, 1972; Hamilton, 2003; Burns *et al.,* 2005).

Water quality degradation in Lake Rotorua has been documented since the early 12th Century, with major eutrophication problems recognised by the 1920s and intensified during the latter half of the century (Hamilton, 2003). Historical direct sewage discharges to the lake

contributed substantial nutrient inputs before diversion in the late 1980s, and recovery from these legacy loads is expected to occur over decades to even centuries for the water column and sediments, respectively (Hamilton, 2003). Contemporary nutrient pressures are dominated by agricultural runoff, groundwater inputs, and internal loading associated with sediment release during stratification events (Mueller *et al.*, 2015).

Figure 1. An algal bloom observed at the Hannah's Bay site of Lake Rotorua during fieldwork. Both images were captured from the jetty on the 24th of November 2025 (Week 1), on the same day of sampling. Photographs by Kendall Williams.

Cyanobacterial blooms are a recurrent feature of Lake Rotorua (Figure 1), most prominently during the summer period, and have resulted in lake closures, health warnings,

and negative impacts on recreational, cultural, and tourism values (Burns *et al.,* 2005; Cotterill *et al.,* 2019). In response, a monitoring programme has been operated by Te Arawa Lakes Trust (TALT) since 20 January 2025 to the present day as part of the LakeCast project, involving routine sampling of chl-*a*, nutrients, water clarity, and phytoplankton community composition at multiple nearshore sites using probe and hand-held sensors, as well as buoys.

Study rationale and objectives

While laboratory-based chl-*a* measurements underpin regulatory assessments and long-term trend analyses, there remains a critical need for rapid, site-specific monitoring tools that can resolve short-term bloom dynamics and spatial variability in nearshore environments (Kraft *et al.,* 2025). This knowledge gap is particularly relevant for management initiatives such as LakeCast, a collaborative algal bloom forecasting project led by the University of Waikato in partnership with TALT, which seeks to improve early warning capabilities and decision-support for Lake Rotorua.

The objectives of this study were to **(1)** Quantify algal biomass using gold-standard laboratory chl-*a* analysis across multiple shoreline sites and sampling periods in Lake Rotorua, capturing spatial and temporal variability in nearshore bloom dynamics; and **(2)** Ground-truth a hand-held fluorescence sensor (FluoroQuik) against laboratory chl-*a* measurements to assess its potential utility for rapid, operational monitoring and bloom forecasting in a eutrophic, polymictic lake system.

By integrating high-resolution nearshore sampling with sensor validation, this study aims to support ongoing monitoring programmes and contribute to the development of responsive, evidence-based management strategies for Lake Rotorua and similar lake systems experiencing recurrent algal blooms.

Methods

Fieldwork

Sample Collection and Storage (Mondays)

Water samples were collected from nine shoreline sites around Lake Rotorua, Bay of Plenty, New Zealand, over summer 2025-2026 (Figure 2). These were selected to align with long-term monitoring locations used by the Bay of Plenty Regional Council (BoPRC), allowing comparability with existing datasets and coordination with TALT. Sampling occurred ~weekly from the 24th of November 2025 to the 12th of January 2026, with six weeks of sampling in total. Moving anticlockwise around the lake, the sampling sites were: **Hannah's Bay** (−38.1128279, 176.3084753), Te Pōhue (−38.0696574, 176.3264715), **Ōhau Channel** (−38.0454842, 176.3239633), Hamurana East (−38.0359914, 176.3085901), **Hamurana Bridge** (−38.0327511, 176.2590061), Hamurana West (−38.0347483, 176.2399933), Ngongotahā river mouth (hereafter Awahou (Tarimano)) (−38.0489922, 176.2231210), **Ngongotahā** (10 Reeme St) (−38.0742228, 176.2163236), and Koutu (private site) (−38.1150131, 176.2395077). In bold are the sites monitored by the BoPRC, and therefore are of key management interest.

Figure 2. Map of Lake Rotorua, New Zealand, showing the 9 shoreline sampling locations. Base imagery sourced from Google Earth.

At each site, surface water (~10 cm depth) was collected using a clean 4 L plastic bucket, filled to approximately full capacity, and gently swirled to mix the sample and disperse algal colonies. When shoreline access infrastructure (e.g., jetties) was unavailable, half-length waders were used to safely collect water samples. One sample was collected per site per manual sampling event (the five weeks after the pilot week), with replicate samples collected only during the initial pilot sampling period. A 60 mL plastic syringe, rinsed twice with sample water, was used to draw 20-30 mL of water (depending on bloom intensity), which was immediately filtered through a 25 mm glass-fibre filter (Whatman GF/C or GC-50; nominal pore size ~0.5-1.2 µm) housed in an Advantec PP-25 polypropylene filter cartridge (syringe

filter holder). This filtration concentrated chl-*a* for subsequent laboratory analysis (Figure 3, Step 1).

Following filtration, filters were carefully handled using forceps, folded twice with the sample side inward, wrapped in aluminium foil (Figure 3, Step 2), labelled with site, date, and filtration volume metadata, sealed in a zip-lock bag, and stored frozen (−20 °C to −70 °C) in the dark until sample analysis. During fieldwork, filters were kept chilled in an insulated chilly bin (Figure 3, Step 3) and transferred to a laboratory freezer upon return (Figure 3, Step 4). Storage at −20 °C has been shown to preserve chl-*a* integrity for at least one month before extraction (SOP Reference 6.1). Reusable equipment (e.g., filter cartridges and syringes) was rinsed three times with ultrapure or distilled water between sites and after fieldwork to minimise cross-contamination.

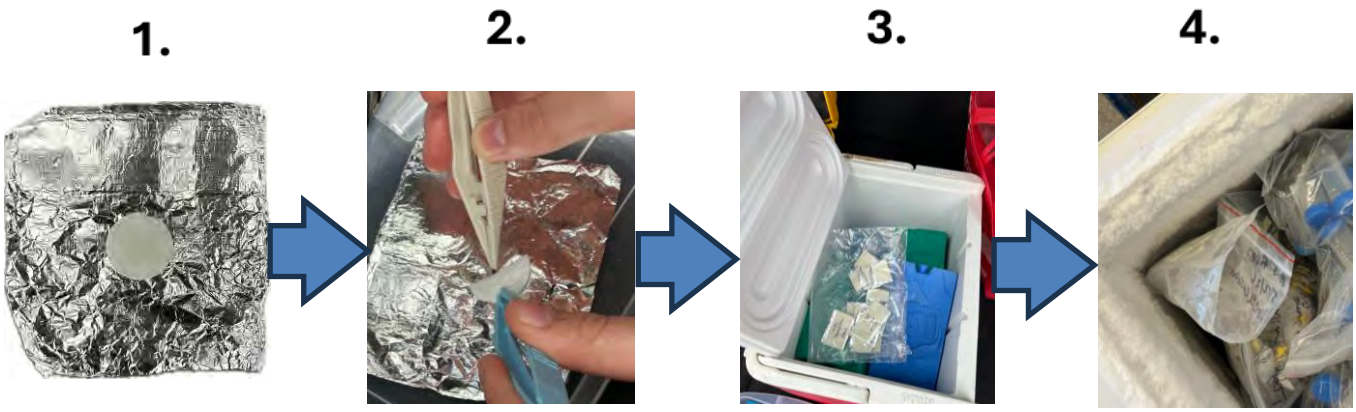

Figure 3. Workflow for handling and storing filtered samples during and after fieldwork. **Step 1:** Using forceps, remove the filter from the cartridge and place it onto a square of aluminium foil. **Step 2**: Fold the filter paper twice with the chlorophyll-*a*–containing surface facing inwards. **Step 3:** Wrap the filter in aluminium foil, label the foil (site, date, sample volume), and place it into a zip-lock bag before storage in a field chilly bin with ice packs. **Step 4:** Upon return to campus, transfer samples from the chilly bin to a chest freezer and store at −20 °C. Photographs by Kendall Williams and Amohia Peka.

Chlorophyll-*a* sampling was conducted across six consecutive weeks (six sampling sessions). The first week served as a pilot trial, during which two replicate samples per site (n = 18) were collected to assess equipment performance and within-site variability. The subsequent five weeks consisted of routine sampling conducted every Monday, with one sample collected per site. In total, 63 chlorophyll-*a* samples were collected (9 sites * 5 weeks + 9 sites * 1 week * 2 reps).

Figure 4. Te Arawa Lakes Trust employee Amohia Peka using the handheld FluoroQuik fluorometer during field sampling for in situ chlorophyll-*a* measurements. Photograph by Kendall Williams.

On each sampling day, handheld fluorescence sensor (i.e., the FluoroQuik) measurements were also taken to compare to laboratory chlorophyll-*a* samples. To understand instrument variability, FluoroQuik measurements were taken using two identical models of the FluoroQuik (labelled A and B) by Amohia Peka (TALT) (Figure 4). For each FluoroQuik instrument, there were 3 replicate measurements taken per site which were later averaged for data analysis.

Laboratory analysis of chl-*a*

Chlorophyll-*a* extraction and analysis were performed fortnightly, typically on the Tuesday and Wednesday following alternate sampling weeks, with a 24-hour delay prior to analysis to allow pigment stabilisation.

Reagent Preparation

All reagents for chl-*a* analysis were prepared using ultrapure water. A saturated magnesium carbonate ($MgCO_3$) solution was made by adding 10 g $MgCO_3$ to 1 L ultrapure water, mixing thoroughly, and allowing the mixture to settle for at least 48 h before decanting the clear supernatant into a clean container.

Buffered acetone (90% v/v) was prepared by combining 900 mL of analytical-grade acetone with 100 mL of saturated $MgCO_3$ solution into a labelled 1 L solution bottle and mixing. Any precipitate material was avoided during use.

A 0.1 N hydrochloric acid (HCl) solution was prepared by adding 0.85 mL of concentrated HCl to approximately 50 mL of ultrapure (distilled) water, then making up to 100 mL total volume. Acid preparation was conducted in a fume hood while wearing appropriate personal protective equipment (e.g., nitrile gloves, lab coat, and eye protection).

Chlorophyll-a Extraction (Tuesdays)

This procedure followed the HECS-HS-S-0234 Chlorophyll-*a* Fluorometric Determination SOP. Extractions were performed under low-light conditions to minimise pigment degradation. The overall extraction setup is shown in Figure 5. Frozen filters were removed from storage and placed into labelled 50 mL screw-cap centrifuge tubes. Each filter was ground into a slurry with 5 mL of buffered acetone (5 mL pipette) using a homogeniser

(Ozito RTG-920VK Rotary Tool) for 2-4 seconds, after which an additional 5 mL of buffered acetone was added to bring the final extraction volume to 10 mL. The homogeniser probe was rinsed with buffered acetone and wiped off in between samples to prevent cross-contamination, with waste solvent collected in a designated container.

Samples were capped and kept covered with aluminium foil to avoid light exposure throughout processing. Extracts were steeped for 2–24 hr at 4 °C in the dark (a duration sufficient for efficient chl-*a* extraction), with tubes shaken at least once during this period. Steeping time varied depending on the interval between extraction and analysis.

Figure 5. Chlorophyll-*a* extraction setup in a laboratory fume hood, showing samples on a rack, homogeniser, pipettes, and buffered acetone used to produce the supernatant. Samples were kept cold on an icepack during processing, with beakers for waste collection and absorbent materials for cleanup. Once homogenised, samples were kept in the dark (covered in aluminium foil) and steeped cold.

Fluorometric Analysis (Wednesdays)

Following the 2–24 hr steeping, tubes were shaken vigorously and centrifuged at 3300 RPM for 10 minutes using a high-brake setting to isolate extractant liquid from the filter particles. The supernatant was allowed to equilibrate to room temperature (~30 min) in the dark

before analysis. Chlorophyll-*a* concentrations were determined using a Turner Designs 10AU fluorometer (Figure 6). The fluorometer was powered on and allowed to warm up for at least 15 min before measurements were taken. Each chl-*a* sample was analysed by pipetting 5 mL of the supernatant into a clean cuvette for an initial reading, followed by acidification and a second reading. New cuvettes were used and discarded after each sample to avoid cross-contamination.

Figure 6. Photo of the Turner Designs 10AU fluorometer used for all laboratory chlorophyll-*a* analyses in this study. Photo taken by Kendall Williams.

A blank reading was first obtained using 5 mL of 90% buffered acetone. The exterior of the cuvette was wiped clean with a Kimwipe™ tissue before measurement. Fluorescence readings were recorded by inserting the cuvette into the fluorometer, covering the chamber, and pressing the start button (‘*’) until “DONE” was displayed.

After the initial blank, 150 µL of 0.1 N HCl (hydrochloric acid) was added to the cuvette (0.2 mL pipette), gently mixed using a glass stirring rod, and left to stand for 90 s before recording a second reading. This acidification step corrects for interference from pheophytin, a degradation product of chl-*a*.

If fluorescence exceeded the instrument's detection range (“OVER”), samples were diluted with buffered acetone, and the dilution factor was recorded. During intense bloom conditions, dilutions up to 3:2 (sample: acetone) were required to obtain readable values. The general fluorometric analysis setup is shown in Figure 7.

Figure 7. Chlorophyll-*a* analysis setup in a laboratory fume hood, showing aluminium-covered centrifuged samples on a rack, cuvettes in a cuvette holder, pipettes and tips, HCl for acidification and blanking, and buffered acetone for dilutions and blanking. Samples were kept in the dark for the duration of analysis, with beakers for waste collection and absorbent materials for cleanup. Taken by Kendall Williams.

Calculations

Chlorophyll-*a* concentration (µg L^{-1}) was calculated from fluorescence readings before and after acidification using the following equation:

where:

$$\text{Chl-a} = F_s \left(\frac{r}{r-1}\right)(R_b - R_a)\left(\frac{V_e}{V_f}\right)\left(\frac{df}{1000}\right)$$

- F_s = fluorometer response factor (from calibration)
- r = acidification coefficient (from calibration sheet)
- R_a = unacidified sample reading minus blank
- R_b = acidified sample reading minus blank
- V_e = extraction volume (10 mL)
- V_f= volume of water filtered (L)
- df = dilution factor

Bloom definition

Calculated chl-*a* concentrations were classified as high and representative of bloom conditions when they exceeded the NPS-FM Band A maximum threshold of 10 µg L^{-1} (Ministry for the Environment, 2025). This threshold represents the upper limit of best-practice ecological condition (i.e., a good ecological state rather than an absence of algae), beyond which algal biomass is no longer considered consistent with high water quality. Exceedance of this value, therefore, indicates a departure from a minimally enriched state and the onset of ecologically meaningful bloom conditions, even in the absence of conspicuous surface scums. Using the Band A maximum provides a precautionary and nationally standardised benchmark that enables early detection of bloom development and supports improved monitoring and management of potential ecological and recreational impacts.

Equipment and Safety

All fieldwork was conducted under an approved field notification and Hazard Management Plan (HMP), with appropriate authorisation obtained through required inductions and University fleet vehicle approval. All laboratory work involving acetone and acids was carried out in a fume hood while wearing nitrile gloves, a laboratory coat, and safety glasses. The centrifuge and fluorometer were checked for electrical safety before use. Waste acetone was collected in designated non-chlorinated solvent waste containers, and glassware and reusable equipment were rinsed three times with ultrapure water after use.

Filtered volumes were recorded in the field for all samples. Laboratory extraction, calibration, and fluorometric analysis followed standard chl-*a* protocols (SOP Reference 6.1) and included procedural blanks and duplicate samples to assess analytical precision and pigment stability during frozen storage. All laboratory work complied with the University of Waikato and the School of Science safety requirements.

Data analysis

Data processing

Field and laboratory chl-*a* data were initially recorded in Microsoft Excel spreadsheets (including calculations) and compiled with associated metadata (site, date, week, and FluoroQuik measurements) using Google Sheets to enable data collation and quality control. The final dataset was exported as a comma-separated values (CSV) file and imported into R.

All analyses were conducted in R version 4.2.2 (R Core Team, 2022) using RStudio (RStudio Team, 2022). Data formatting and manipulation were performed using the *dplyr* package (Wickham *et al.*, 2025). Data cleaning procedures included removal of missing values,

standardisation of site names, ordering of sampling sites as factors, and conversion of date fields into appropriate date formats. Site categories were explicitly defined as ordered factors to ensure consistency across analyses and figures.

Where replicate measurements were available, values were averaged to produce a single observation per site–week. This included averaging replicate laboratory samples collected during the first week of sampling and averaging FluoroQuik measurements for each week, where instruments A and B each collected three replicates per site. This approach ensured one value per site-week observation and avoided bias arising from uneven replication.

Data analysis

Linear regression analyses were used to quantify relationships between laboratory-derived chl-*a* concentrations and FluoroQuik measurements, both globally across all sites and weeks and for individual sites (local). Separate regression models were also fitted for low (≤10 μg L^{-1}) and high (>10 μg L^{-1}) chlorophyll-*a* concentration ranges to assess potential non-linear responses and threshold effects in sensor performance.

Model performance was evaluated using coefficient estimates, coefficient of determination (R^2), and analysis of variance (ANOVA) to test the statistical significance of regression relationships.

Data visualisation

All plots were generated using *ggplot2* (Wickham, 2016), while *tibble* (Müller & Wickham, 2026), *cowplot* (Wilke, 2025), and *patchwork* (Pedersen, 2025) were used for data manipulation and combining figures. Visualisations included boxplots and time-series plots to examine spatial and temporal differences among sites and sampling weeks, as well as scatter plots with linear regressions (both global and site-specific) to compare FluoroQuik

measurements with laboratory chlorophyll-*a* concentrations. These figures provided a clear representation of variation across sites and weeks and supported the interpretation of statistical analyses. Necessary statistical information (e.g., *p*-value, R^2, mean, and standard deviations) was compiled into two tables for easy readability and comprehension of the visual plots.

Results

Objective 1: Laboratory Chlorophyll-a analysis demonstrates spatial and temporal variability in algal biomass for Lake Rotorua

Laboratory-measured chl-*a* concentrations exhibited substantial temporal and spatial variability across the six-week monitoring period (Figures 8–10, Tables 1–2). Concentrations of chl-*a* varied across sites over time, highlighting both temporal shifts in overall biomass and site-specific episodic peaks and troughs (Figure 8). Several sites, including Awahou (Tarimano), Ōhau Channel, and Hamurana (Bridge), all on the northern side of Lake Rotorua, frequently (at least 3/6 weeks) exceeded the 10 µg L^{-1} NPS-FM Band A maximum threshold (Ministry for the Environment, 2025).

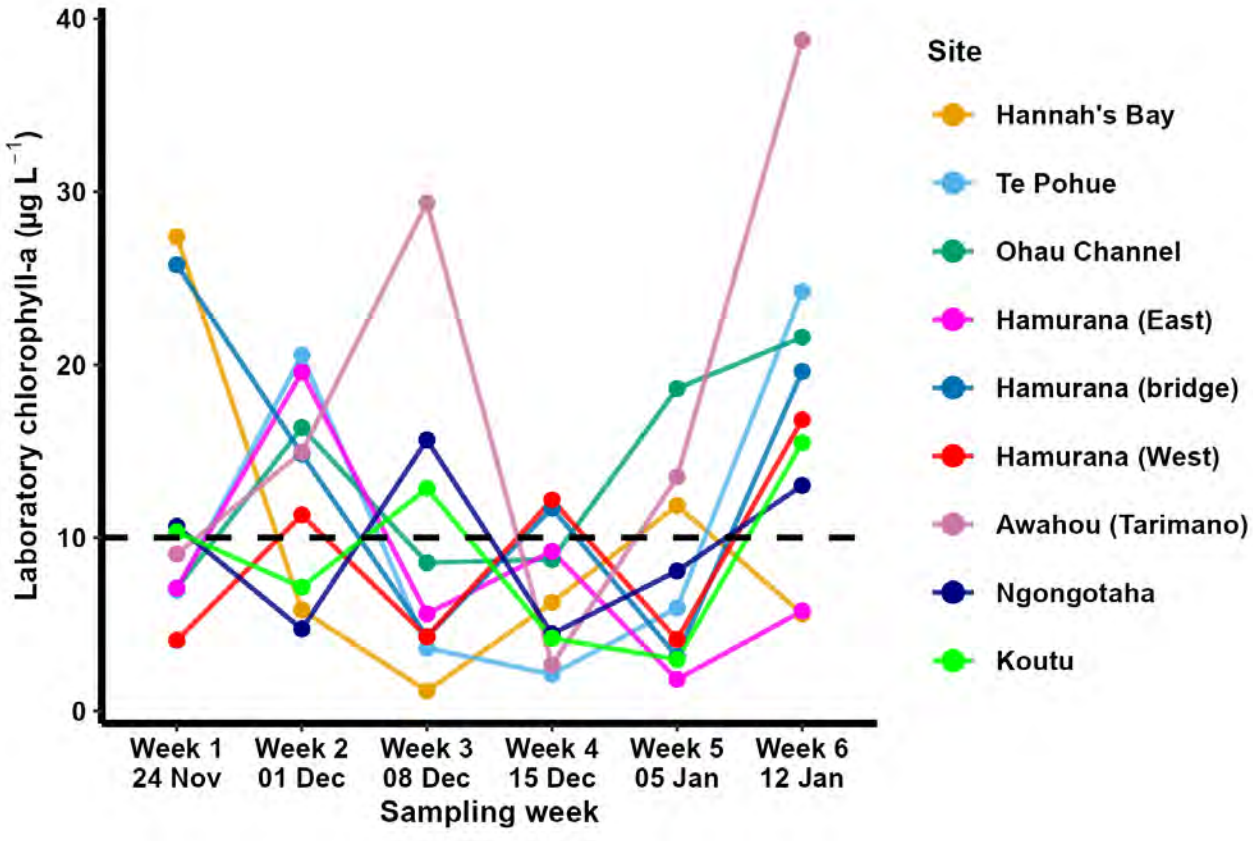

Figure 8. Time series of laboratory chlorophyll-*a* (µg L^{-1}) across nine sites around Lake Rotorua over six weeks of sampling. Coloured points and lines represent individual site-week observations. The dotted black line represents the 10 µg L^{-1} bloom threshold.

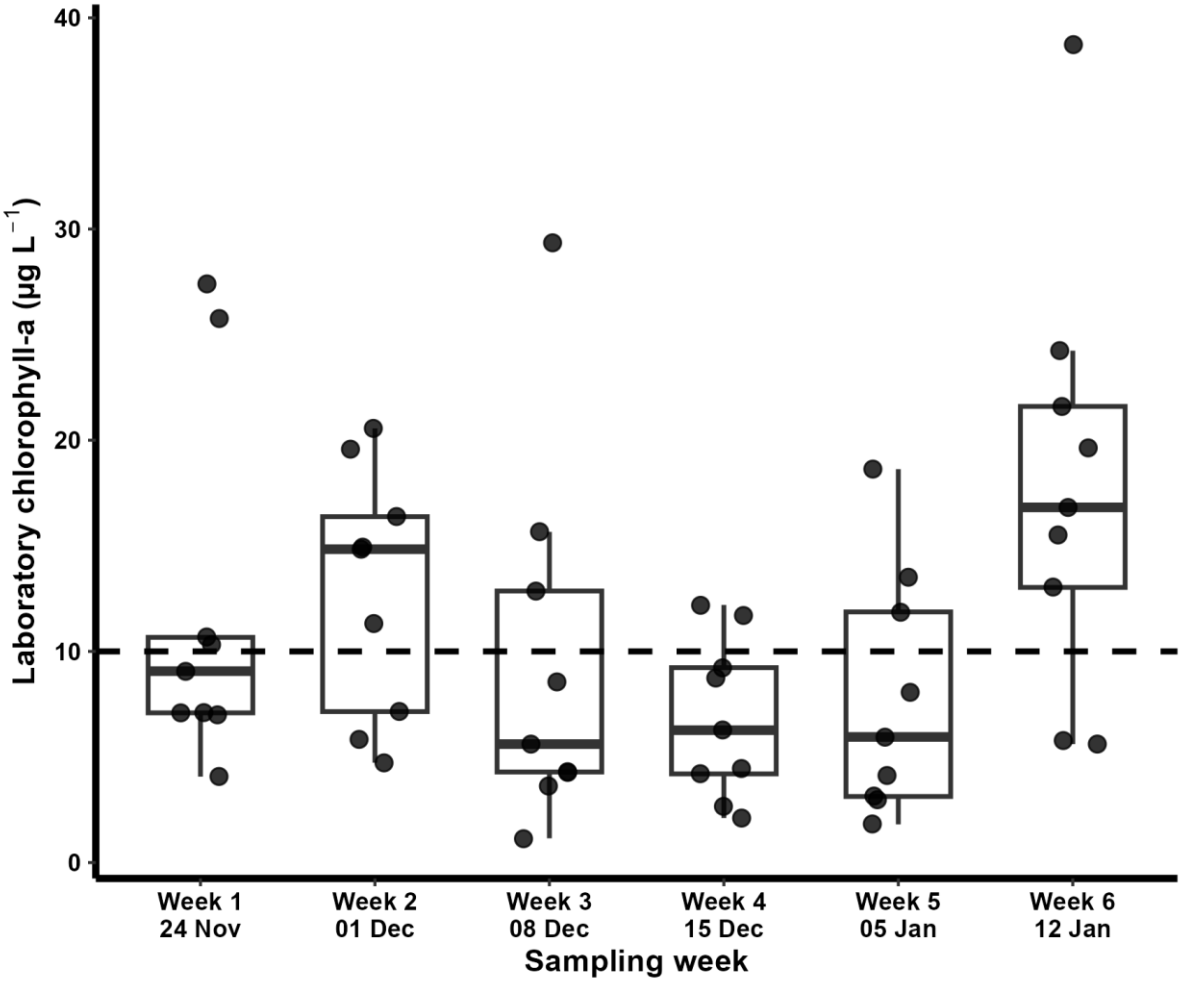

Figure 9. Box plot showing weekly variation in laboratory-measured chlorophyll-*a* concentrations (µg L^{-1}) across 9 sites around Lake Rotorua, New Zealand. The dotted black line represents the 10 µg L^{-1} NPS-FM threshold for the Band A maximum chl-*a* (Ministry for the Environment, 2025).

In contrast, more southerly sites such as Hannah's Bay (excluding Week 1, max = 27.41 µg L^{-1}), Ngongotahā, and Koutu remained near or below 10 µg L^{-1} for Weeks 1, 3, and 6, but under 20 µg L^{-1} for all six (Table 2). Interestingly, Hamurana West and East exhibited lower overall chl-*a* concentrations than the neighbouring Hamurana Bridge site, reaching maximum chl-*a* concentrations of 16.8 and 19.5 µg L^{-1}, respectively. Te Pōhue on the east was very divided in chl-*a* concentrations throughout the weeks, with Weeks 2 and 6 having chl-*a* concentrations > 20 µg L^{-1}, and the remaining well below 10 µg L^{-1}.

Table 1. Summary statistics of Chlorophyll-a concentration (μg L^{-1}) across nine sampling sites, showing minimum (Min), first quartile (Q1), median, third quartile (Q3), maximum (Max), mean, standard deviation (SD), and sample size (n) for each week (n = 6 weeks per site). Site orientation relative to the lake is indicated in parentheses.

Site	Min	Q1	Median	Q3	Max	Mean	SD	n
Hannah's Bay (SE)	1.15	5.665	6.050	10.470	27.41	9.690	9.327	6
Te Pōhue (E)	2.11	4.210	6.465	17.165	24.24	10.578	9.388	6
Ōhau Channel (NE)	7.09	8.613	2.560	118.068	21.60	13.502	6.136	6
Hamurana (East) (NE)	1.81	5.650	6.430	8.695	19.57	8.180	6.083	6
Hamurana (bridge) (N)	3.13	6.145	13.275	18.425	25.78	13.228	8.777	6
Hamurana (West) (NW)	4.07	4.163	7.805	11.980	16.82	8.803	5.419	6
Awahou (Tarimano) (NW)	2.67	10.179	14.235	25.750	38.75	18.051	13.443	6
Ngongotahā (W)	4.45	5.568	9.373	12.439	15.66	9.436	4.517	6
Koutu (SW)	2.97	4.938	8.740	12.228	15.50	8.835	4.931	6

Table 2. Summary statistics of Chlorophyll-a concentration (μg L^{-1}) across six weeks, showing minimum (Min), first quartile (Q1), median, third quartile (Q3), maximum (Max), mean, standard deviation (SD), and sample size (n) for each week (n = 9 sites per week).

Week	Min	Q1	Median	Q3	Max	Mean	SD	n
1	4.07	7.09	9.065	10.665	27.41	12.053	8.491	9
2	4.73	7.15	14.840	16.380	20.56	12.814	5.868	9
3	1.15	4.29	5.610	12.860	29.35	9.490	8.787	9
4	2.11	4.20	6.270	9.230	12.20	6.842	3.784	9
5	1.81	3.13	5.950	11.870	18.63	7.787	5.751	9
6	5.61	13.03	16.820	21.600	38.75	17.882	10.127	9

Weekly patterns (Figure 9) showed fluctuations in algal biomass and bloom dynamics across the monitoring period. Week 1 had moderately elevated concentrations (median = 9.07 μg L^{-1}, mean = 12.05 μg L^{-1}), which increased in Week 2 (median = 14.84 μg L^{-1}, mean = 12.81 μg L^{-1}) (Table 2). Weeks 3–5 were lower (medians ≤ 6.27 μg L^{-1}), although high biomass at some sites persisted, particularly in Week 3 (Awahou (Tarimano); max = 29.35 μg L^{-1}). Week 4 exhibited the lowest overall concentrations and variability (mean = 6.84 μg L^{-1}, SD = 3.78), while Week 5 showed a small increase in maximum observed biomass (Ōhau Channel, 18.63 μg L^{-1}), but not median biomass (5.95 μg L^{-1}). Week 6 showed a pronounced increase (median = 16.82 μg L^{-1}, mean = 17.88 μg L^{-1}) with the highest maximum (Awahou (Tarimano) = 38.75 μg L^{-1}) and variability (SD = 10.13), indicating late-period intensification of algal biomass (i.e., a bloom). Consistent sampling (n = 9 per week) confirms these patterns reflect genuine temporal changes rather than sampling bias.

Table 3. Weekly laboratory-measured chlorophyll-*a* concentrations (μg L^{-1}) at nine sampling sites around Lake Rotorua, New Zealand, across six consecutive weeks (W1–W6). Values represent site-specific observations, with site orientation relative to the lake indicated in parentheses. Exceedances of the 10 μg L^{-1} bloom threshold are in bold. Wind direction and peak gusts (km/h) are included for each week.

Week	**W1**	**W2**	**W3**	**W4**	**W5**	**W6**
Site (Direction)						
Hannah's Bay (SE)	**27.41**	5.83	1.15	6.27	**11.87**	5.61
Te Pōhue (E)	6.98	**20.56**	3.63	2.11	5.95	**24.24**
Ōhau Channel (NE)	7.09	**16.38**	8.57	8.74	**18.63**	**21.60**
Hamurana (East) (NE)	7.09	**19.57**	5.61	9.23	1.81	5.77
Hamurana (Bridge) (N)	**25.78**	**14.84**	4.29	**11.71**	3.13	**19.62**
Hamurana (West) (NW)	4.07	**11.32**	4.29	**12.20**	4.12	**16.82**
Awahou (Tarimano) (NW)	9.07	**14.95**	**29.35**	2.67	**13.52**	**38.75**
Ngongotahā (W)	**10.67**	4.73	**15.66**	4.45	8.08	**13.03**
Koutu (SW)	**10.33**	7.15	**12.86**	4.20	2.97	**15.50**
Wind direction, peak gust (km/h)	NW, 17	W, 48	NNE, 26	NNE, 32	NNE, 34	WSW, 37

Note. Wind gusts based on 12:00-18:00 Monday averages (Time and Date AS, 2026).

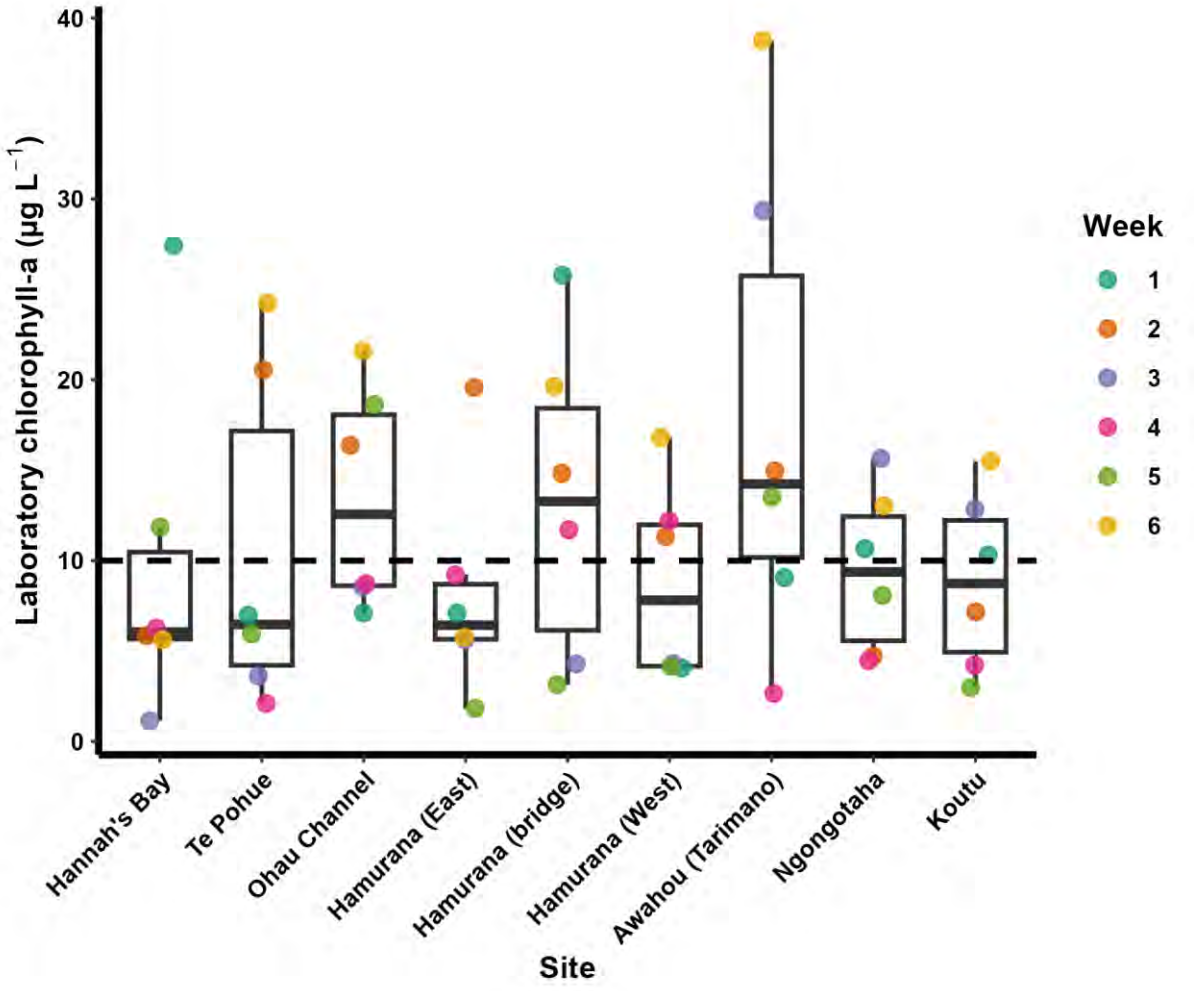

Figure 10. Box plot showing site variation in laboratory-measured chlorophyll-*a* concentrations (µg L^{-1}) over 6 weeks around Lake Rotorua, New Zealand. Coloured points represent site-week observations. The dotted black line represents the 10 µg L^{-1} NPS-FM threshold for the Band A maximum chl-*a* (Ministry for the Environment, 2025).

Spatial variation among sites was also evident in chl-*a* concentrations, alongside pronounced temporal variability across the sampling period (Figure 10; Table 3). Overall mean chl-*a* concentrations ranged from 8.18 µg L^{-1} at Hamurana (East) to 18.05 µg L^{-1} at Awahou (Tarimano), which also exhibited the greatest spread (range = 36.08 µg L^{-1}) and variability (SD = 13.44) (Table 2). In contrast, Ngongotahā and Koutu showed comparatively low overall variability (SD ≈ 4.5 µg L^{-1}).

Temporal variability was characterised by distinct weekly pulses, with broadly elevated concentrations during Weeks 2 and 6 and more subdued chl-*a* levels through the mid-period (Weeks 3-5) (Figure 10). Extreme values were spatially clustered at specific shoreline sites rather than occurring synchronously across the lake. Awahou (Tarimano) exhibited the most dynamic behaviour, with a pronounced bloom event in Week 3 (29.35 µg L^{-1}) and Week 6 (38.75 µg L^{-1}), representing the highest concentrations observed during the study (Table 2; Table 3). Similarly, Te Pōhue and Hamurana (Bridge) displayed pulsed high concentrations, particularly during Weeks 1 (Hamurana Bridge, max = 25.78 µg L^{-1}), 2 (Te Pōhue, max = 20.56 µg L^{-1}), and 6 (Te Pōhue = 24.24 µg L^{-1}, Hamurana Bridge = 19.62 µg L^{-1}), consistent with episodic bloom development rather than sustained elevated biomass.

Elevated central tendencies were observed at Awahou (Tarimano), Hamurana (Bridge), and Ōhau Channel, with median values exceeding our bloom threshold (medians ≈ 12-14 µg L^{-1}) (Figure 10). At Hamurana (Bridge), the disparity between median (13.28 µg L^{-1}) and mean values (23.23 µg L^{-1}) reflects the influence of short-lived high-biomass events. In contrast, Hannah's Bay, Hamurana (East and West), and Koutu generally maintained low to moderate concentrations following early-period peaks, with median values between ~6–9 µg L^{-1}, and minimum values as low as 1.15 µg L^{-1} (Hannah's Bay, Week 3), indicating more stable local conditions. Collectively, the data indicate dynamic, site-specific bloom events rather than a consistent monotonic trend.

Overall, laboratory-measured chl-*a* concentrations were highly variable across both space and time, with pronounced site-specific and episodic bloom dynamics rather than uniform lake-wide trends (Table 3). Collectively, these patterns demonstrate a highly heterogeneous bloom regime across Lake Rotorua, driven by short-lived, site-specific events

and periodic lake-wide increases, highlighting the importance of high-frequency, multi-site monitoring for accurately capturing algal bloom dynamics and associated water quality risks.

Objective 2: Hand-held Fluorescence FluoroQuik sensor reliably detects high-biomass blooms but shows variable performance across sites and low chlorophyll-a concentrations

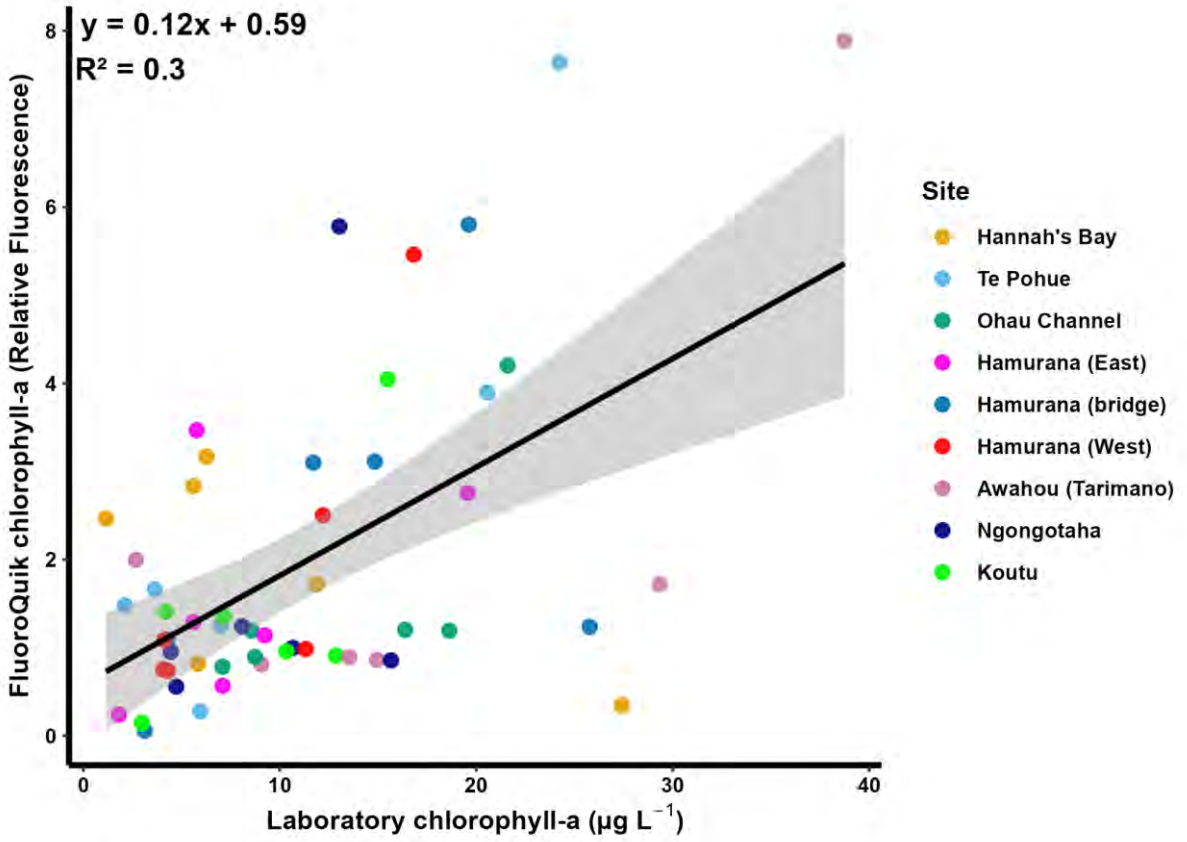

Figure 11. Global linear regression showing the relationship between laboratory-measured chl-*a* (µg L^{-1}) and FluoroQuik (hand-held sensor) chlorophyll-*a* (Relative Units of Fluorescence, RFU) across nine shoreline sites around Lake Rotorua over six weeks of sampling. Points represent individual site–week observations, and the solid line indicates the overall regression ($p < 0.001$).

Laboratory-measured chl-*a* concentrations were positively related to hand-held FluoroQuik relative fluorescence across the full dataset (Figure 11), indicating an overall correspondence between laboratory and sensor-based measurements. The global regression model showed a significant positive relationship (Y = 0.12x + 0.59, $R^2 = 0.30$, $p > 0.0001$),

demonstrating that approximately 30% of the variance in FluoroQuik fluorescence was explained by laboratory chl-*a* concentrations. Although the relationship was statistically significant, the moderate coefficient of determination indicates substantial unexplained variability, suggesting that the strength of correspondence between methods varied across concentration ranges and sites.

When examining relationships below and above the 10 ug/L bloom threshold (Figure 12), contrasting patterns emerged. At low concentrations (< 10 µg L^{-1}, Figure 12a), no relationship was observed between laboratory chl-*a* and FluoroQuik fluorescence (Y = 0x + 1.26, R^2 = 0.0001, p = 0.95), indicating an absence of sensor sensitivity or signal discrimination at low algal biomass levels.

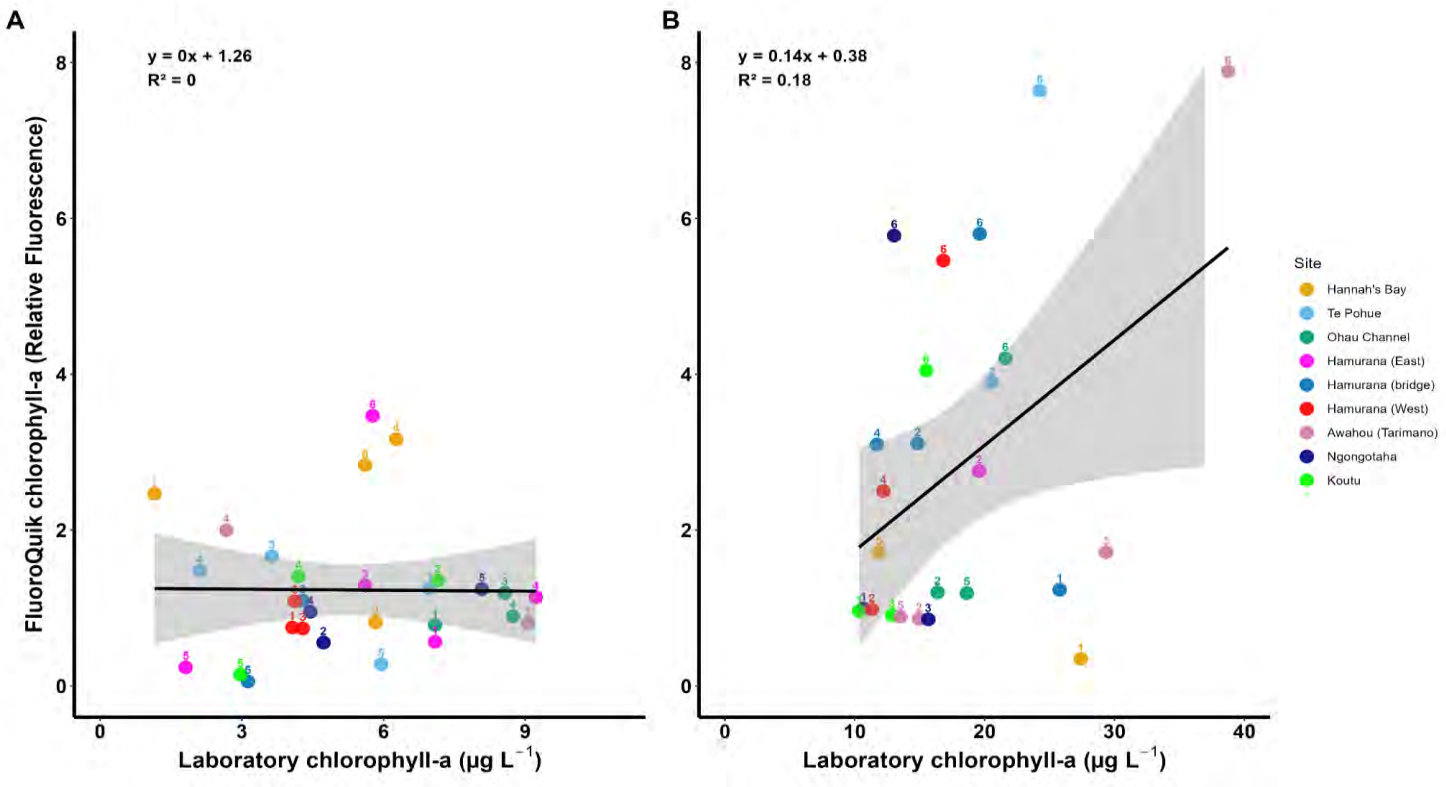

Figure 12. Regression relationships between laboratory-measured chlorophyll-*a* and FluoroQuik relative fluorescence for concentration subsets below (< 10 µg L^{-1}, **A**) and above (≥ 10 µg L^{-1}, **B**) the NPS-FM Band A threshold. Coloured points represent site-specific values, while point numbers represent the specific week observed.

In contrast, at higher concentrations (≥ 10 µg L^{-1}, Figure 12b), a weak but statistically significant positive relationship was detected ($Y = 0.14x + 0.38$, $R^2 = 0.18$, $p = 0.04$), indicating improved sensor responsiveness under elevated biomass conditions. This threshold-dependent response suggests that FluoroQuik performance is concentration-sensitive, with stronger correspondence occurring during bloom conditions (i.e., higher chl-*a* concentrations). Several observations fell outside of the 95% confidence interval of the fitted relationship.

Positive outliers were characterised by elevated FluoroQuik fluorescence (higher than expected) relative to laboratory chl-*a*, suggesting disproportionately strong in situ fluorescence at moderate biomass levels. Moderate laboratory chl-*a* (~15-25 µg L^{-1}) paired with elevated FluoroQick values (~4-8 RFU) predominantly during Week 6 at 5 sites (Koutu, Ngongotahā, Hamurana (West, bridge), and Te Pōhue). Conversely, negative outliers exhibited low FlouroQuik fluorescence despite high laboratory chl-*a* concentrations, consistent with reduced fluorescence efficiency at high biomass, potentially reflecting bloom senescence. High laboratory chl-*a* (~20-30+ µg L^{-1}) paired with low FlouroQuik values (< 1-2 RFU) for specific site-week observations: Week 1 (Hamurana (Bridge), Hannah's Bay), Week 2 (Awahou (Tarimano), Ōhau Channel), Week 3 (Ngongotahā, Awahou (Tarimano), Koutu), and Week 5 (Awahou (Tarimano), Ōhau Channel).

Site-specific regressions (Figure 13, Table 4) further demonstrated strong spatial heterogeneity in sensor–laboratory relationships.

Significant positive relationships were observed at Te Pōhue ($Y = 0.26x - 0.02$, $R^2 = 0.80$, $p = 0.02$; Figure 13b) and Hamurana (West) ($Y = 0.29x - 0.64$, $R^2 = 0.72$, $p = 0.03$; Figure 13f), indicating strong local agreement between FluoroQuik fluorescence and laboratory chl-*a* measurements. Moderate but non-significant relationships were evident at Awahou (Tarimano)

(R^2 = 0.56, p = 0.09; Figure 13g) and Ōhau Channel (R^2 = 0.51, p = 0.11, Figure 13c), suggesting partial correspondence that did not reach statistical significance.

Table 4. Linear regression relationships between laboratory-measured chlorophyll-a concentration (µg L^{-1}) (x) and handheld FluoroQuik relative fluorescence (RFU) (y) for global, threshold-subset, and site-specific models. Significant findings are in bold.

Site/Model	**Regression Equation**	R^2	***P*-value**
Hannah's Bay	Y = -0.08x + 2.71	0.48	0.13
Te Pōhue	Y = 0.26x + -0.02	0.80	**0.02**
Ōhau Channel	Y = 0.15x + -0.46	0.51	0.11
Hamurana (East)	Y = 0.1x + 0.75	0.24	0.33
Hamurana (Bridge)	Y = 0.11x + 0.94	0.22	0.35
Hamurana (West)	Y = 0.29x + - 0.64	0.72	**0.03**
Awahou (Tarimano)	Y = 0.15x + -0.39	0.56	0.09
Ngongotahā	Y = 0.18x + 0.04	0.16	0.43
Koutu	Y = 0.18x + -0.16	0.46	0.14
Low subset (< 10 µg L^{-1})	Y = 0x + 1.26	0.0001	0.95
High subset (≥ 10 µg L^{-1})	Y = 0.14x +0.38	0.18	**0.04**
Global Regression	Y = 0.12x + 0.59	0.30	< **0.001**

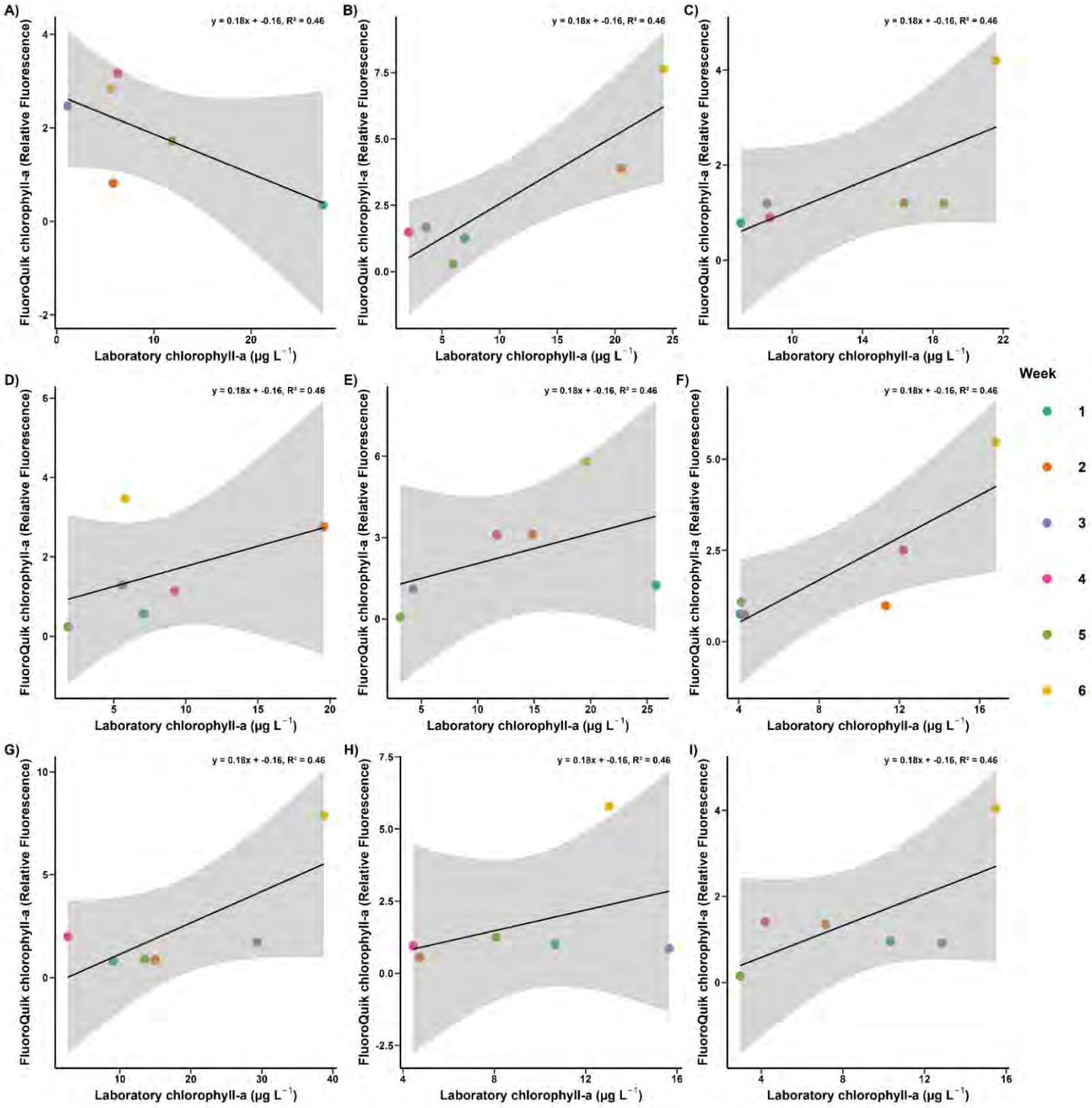

Figure 13. 9-Grid Local site linear regression showing the relationship between laboratory-measured chlorophyll-*a* (µg L^{-1}) and FluoroQuik (hand-held sensor) chl-*a* (RFU) across nine shoreline sites around Lake Rotorua over six weeks of sampling: **A,** Hannah's Bay; **B,** Te Pōhue; **C,** Ōhau Channel; **D,** Hamurana (East); **E,** Hamurana (Bridge); **F,** Hamurana (West); **G,** Awahou (Tarimano); **H,** Ngongotahā; and **I,** Koutu. Coloured points represent individual site–week observations, and the solid line indicates the overall regression ($p < 0.001$).

Other sites, including Hannah's Bay, Hamurana (East), Hamurana (Bridge), Ngongotahā, and Koutu, exhibited weak and non-significant relationships (R^2 = 0.16–0.48, p > 0.13), indicating limited predictive performance of the sensor at these locations. These sites also have lower overall mean chl-*a* values, further supporting my findings that at lower concentrations, the relationship between the FluoroQuik chl-*a* and laboratory chl-*a* is broken.

Although the majority of plots showed observations broadly following the fitted trendlines, four sites exhibited major outliers falling outside the 95% confidence intervals. At Hannah's Bay (Figure 13a), two negative outliers were observed. During Week 2, relatively low FluoroQuik chl-*a* (~1 RFU) was paired with low–moderate laboratory chl-*a* (~6 µg L^{-1}), falling below the regression line. A second negative outlier occurred during Week 1, where high laboratory chl-*a* (~27 µg L^{-1}) was associated with markedly lower-than-expected FluoroQuik chl-*a* (~0.4 RFU), indicating an under-response of FluoroQuik relative to laboratory measurements. Hamurana (East) exhibited a positive outlier during Week 6, characterised by elevated FluoroQuik chl-*a* (~4 RFU) despite low laboratory chl-*a* (~5 µg L^{-1}), falling above the fitted relationship (Figure 13d). Hamurana (West) showed a negative outlier during Week 2, with low FluoroQuik chl-*a* (~0.5 RFU) relative to moderate laboratory chl-*a* (~11 µg L^{-1}), falling below the regression line (Figure 13f). Finally, Ngongotahā displayed a positive outlier in Week 6, where FluoroQuik chl-*a* (~6 RFU) was higher than expected for the corresponding laboratory chl-*a* (~13 µg L^{-1}) (Figure 13h).

Collectively, these results demonstrate that while FluoroQuik fluorescence provides a statistically significant proxy for laboratory chl-*a* at the global scale, its performance is highly concentration-dependent and site-specific. Sensor–laboratory agreement is strongest during high-biomass conditions and at specific sites, whereas low-concentration conditions and

certain locations exhibit weak or absent relationships, highlighting spatial and threshold-based limitations in sensor reliability.

Results Summary

Across the six-week monitoring period, algal biomass in Lake Rotorua exhibited strong spatial and temporal heterogeneity, characterised by short-lived, site-specific bloom events rather than sustained lake-wide trends (Figure 8). Laboratory-measured chl-*a* concentrations varied markedly among weeks and sites, with distinct temporal pulses and episodic peaks that frequently exceeded our bloom definition at selected shoreline locations. The most pronounced blooms were observed during Weeks 2 and 6 (1/12/25 and 12/01/26), with the highest observed concentrations recorded at Awahou (Tarimano), Te Pōhue, and Hamurana (Bridge), while mid-period weeks (Weeks 3–5, 8/12/25–5/01/26) were characterised by generally lower biomass across most sites.

Spatial patterns further indicated persistent differences among sites, with Awahou (Tarimano) exhibiting the highest mean concentrations and greatest variability (mean = 18.1 μg L^{-1}, SD = 13.4; Table 1), reflecting repeated bloom development, whereas sites such as Hannah's Bay, Hamurana (East), and Koutu generally maintained lower and more stable chl-*a* concentrations. Extreme values were temporally clustered and geographically localised, highlighting the episodic nature of bloom formation and the absence of a consistent monotonic increase or decline across the study period.

Ground-truthing of the FluoroQuik hand-held fluorescence sensor against laboratory chl-*a* measurements revealed a statistically significant but moderate overall relationship ($Y = 0.12x + 0.59$, $R^2 = 0.30$, $p > 0.0001$), indicating partial agreement between methods (Figure 11).

The sensors' performance was strongly concentration-dependent, with no detectable relationship at chl-*a* concentrations below 10 μg L^{-1} and a weak but significant positive relationship above this threshold (Figure 12). Furthermore, sensor–laboratory agreement varied substantially among sites, with strong relationships observed at only a subset of locations, while several sites exhibited weak or non-significant correspondence. Together, these findings demonstrate that FluoroQuik fluorescence can reflect elevated algal biomass under bloom conditions, although its reliability is limited under low-biomass conditions and is highly site-specific.

Discussion

Objective 1: Disturbance-driven and spatially structured bloom dynamics in a polymictic eutrophic lake

The bloom dynamics observed in Lake Rotorua align with a disturbance-driven model of phytoplankton proliferation rather than a gradual seasonal accumulation of biomass. There was a clear episodic, pulsed, and non-linear behaviour recorded during the six weeks of sampling (Figure 8). In general, repeated cycles of stratification and mixing can create short windows of nutrient availability, particularly through internal phosphorus release under hypoxic bottom-water conditions (Rutherford *et al*, 1996; Hamilton, 2003). When these pulses coincide with favourable light and temperature conditions, rapid phytoplankton growth can occur over days to weeks, producing the sharp biomass peaks observed during Weeks 2 and 6, alongside extreme site-specific events such as those observed at Awahou (Tarimano), with no consistent increasing or decreasing trend through time (Figure 8). The absence of a monotonic temporal trajectory across the monitoring period suggests that bloom formation was governed by interacting physical and biogeochemical triggers, rather than progressive nutrient build-up alone.

Lake Rotorua's geomorphology and catchment characteristics likely amplify this pulsed behaviour. The lake's high catchment-to-volume ratio, extensive pastoral land use, and legacy nutrient enrichment mean that both external loading (through inflows and groundwater) and internal loading (through sediments) remain substantial drivers of trophic state (Hamilton, 2003; Mueller *et al.,* 2015). Even with nutrient mitigation strategies in place (e.g., alum-dosing), eutrophic systems often exhibit a lag where recovery is slow following reduced nutrient inputs due to sediment nutrient reservoirs and feedback mechanisms promoting further algal growth (Moss, 1998). This legacy effect may underpin the rapid biomass response seen during discrete weeks, reflecting internal nutrient mobilisation rather than new catchment

inputs alone. The temporal structure observed may indicate this occurring, with algal biomass being driven primarily by short-lived bloom events rather than slow accumulation processes. Event-based triggers could include rainfall, catchment runoff, inflows, sediment resuspension, and physical mixing events.

The strong spatial clustering of bloom maxima (and more frequent exceedances of the 10 μg L^{-1} bloom threshold) at northern inflow- (Awahou (Tarimano), Hamurana (Bridge)) and outflow- (Ōhau Channel) associated sites highlights the importance of hydrological exchange zones in structuring nearshore variability. Elevated chl-*a* at these locations underscores how hydrological connectivity influences bloom patterns, with the inflowing Awahou (Tarimano) and Hamurana (Bridge) acting as nutrient (e.g., nitrogen and phosphorus) delivery pathways from the surrounding catchment, and the outflowing Ōhau Channel primarily reflecting the transport and redistribution of internally generated lake biomass. These connected zones (i.e., hotspots) experience altered flow regimes, residence times, turbulence, and thermal structure—all of which shape phytoplankton growth conditions (Hamilton, 2003; Wu *et al.*, 2023). The consistently elevated medians at these stream-associated sites suggest not only episodic bloom peaks but sustained higher baseline exposure to bloom risk. This supports the idea that nearshore areas adjacent to major hydrological exchange points can function as semi-distinct ecological parts within the broader lake system, where local hydrodynamics amplify bloom dynamics. In contrast, Hannah's Bay and Hamurana (East) generally maintained lower concentrations, suggesting comparatively more stable local conditions. This uneven spatial distribution of bloom risk has direct implications for risk-based management, spatial zoning, and targeted mitigation strategies focused on hydrologically connected shoreline zones.

Additionally, bloom events were not uniformly distributed temporally, revealing a distinction between lake-wide pulses and localised bloom development. Some events, such as during Week 6, were characterised by increased biomass across multiple sites. Importantly,

ecological risk was driven more by variability and extremes than by mean conditions, as demonstrated by high standard deviations, extreme maxima, and wide distributions in Figures 9 and 10. These findings reinforce the interpretation of blooms as disturbance events rather than background ecological states, with impacts driven by short-lived but intense biomass pulses.

Wind patterns and local site exposure further contributed to the spatial heterogeneity of nearshore algal blooms in Lake Rotorua (Table 3). In shallow polymictic systems, wind both resuspends sediments–increasing turbidity and releasing bound phosphorus–and redistributes buoyant cyanobacteria toward downwind margins (Reynolds *et al.,* 2002; Deng *et al.,* 2016). Consequently, biomass accumulation along certain horizons may reflect physical concentration processes rather than in situ growth alone. The coexistence of lake-wide pulses (e.g., Week 6) and highly localised peaks (e.g., Awahou (Tarimano) Week 3) suggests a dual-scale forcing regime: system-scale meteorological drivers interacting with site-specific hydrology and morphology. Wind data were obtained from the Time and Data historic weather records for Rotorua (12–6 pm Monday averages; Time and Data AS, 2026), and site-specific observations of surface conditions, such as ripples, waves, water colour, and floating debris, were recorded during sampling. Sheltered sites such as Hannah's Bay (SE) and Te Pōhue (E) experienced relatively low wind influence, including NW 17 km/h in Week 1, with generally calm ripples and lightly coloured water, which corresponded with high early-season chl-*a* concentrations (Hannah's Bay 27.41 μg L^{-1}, Week 1; Te Pōhue 20.56 μg L^{-1}, Week 2). In contrast, exposed sites, including Awahou (Tarimano, NW), Ngongotahā (W), Hamurana (West, NW), and Koutu (SW), were subject to higher wind activity, with peak gusts up to 48 km/h (W, Week 2), 26–34 km/h (NNE, Weeks 3–5), and 37 km/h (WSW, Week 6). Observational notes indicated increased wave action, murkier water, and occasional floating debris at these exposed sites during windy periods. At these sites, stronger winds coincided with lower or more variable chl-

a concentrations, likely due to enhanced mixing and redistribution of algal biomass (e.g., Ngongotahā 4.73 μg L^{-1}, Week 2; Koutu 2.97 μg L^{-1}, Week 5). Nonetheless, bloom peaks still occurred during calmer or moderately windy periods, such as Awahou (Tarimano) in Week 3 (29.35 μg L^{-1}) and Week 6 (38.75 μg L^{-1}), highlighting the role of intermittent calm intervals in promoting high-biomass accumulation. Semi-exposed sites, such as Ōhau Channel (NE) and Hamurana Bridge (N), displayed intermediate patterns, with moderate wave action and NNE winds (26–32 km/h) producing chl-*a* peaks during locally calmer conditions (Ōhau Channel 21.60 μg L^{-1}, Week 6). Notably, dead guppy fish were observed at Ōhau Channel during Week 3, despite moderate chl-*a* concentrations (~8 μg L^{-1}), suggesting that mortality may have been a delayed response to the higher biomass observed in Week 2 (~16 μg L^{-1}), potentially reflecting the lagged effects of prior bloom-induced stress. Overall, these observations suggest that calm to moderate wind conditions favour bloom formation, particularly at sheltered and semi-sheltered sites, whereas sustained or strong winds at exposed sites increase mixing, limiting nearshore chl-*a* accumulation and creating greater temporal variability in bloom magnitude.

Importantly, the episodic exceedance of the 10 μg L^{-1} bloom threshold demonstrates that ecological risk is governed more by extremes and variability than by mean conditions. High standard deviations and wide interquartile ranges indicate a system characterised by instability and rapid transitions between moderate and bloom states. This pattern is typical of eutrophic lakes approaching or oscillating around ecological tipping points, where small environmental perturbations can trigger disproportionate biomass responses (Moss, 1998; Paerl *et al.,* 2018). From a management perspective, reliance on median or seasonal averages may therefore underestimate short-term exposure risks relevant to recreation and public health.

Collectively, these findings reinforce the necessity of shoreline-focused, high-frequency monitoring capable of capturing both lake-wide pulses and localised bloom events.

Nearshore zones represent the interface between ecological processes and human use, and they are disproportionately influenced by hydrodynamic accumulation and inflow-driven nutrient pulses (Kraft et al., 2025). The strong spatial asynchrony observed here demonstrates that single-site or pelagic monitoring frameworks would fail to capture the true magnitude and variability of bloom risk in Lake Rotorua.

Objective 2: Optical and ecological constraints on FluoroQuik fluorescence-based biomass estimation against ground-truth laboratory extraction

Ground-truthing of the FluoroQuik hand-held fluorescence sensor demonstrates that it is a conditionally reliable proxy for laboratory-measured chl-*a* rather than a universally accurate replacement. The moderate global relationship between FluoroQuik fluorescence and laboratory chl-*a* reflects both the potential and the inherent limitations of in situ fluorescence sensing (R^2 = 0.30, Figure 11). This suggests that sensor performance varies substantially across concentration ranges and sites, with significant and strong relationships only occurring at selected sites (Te Pōhue, Hamurana (West), Awahou (Tarimano), Table 4. Fluorescence-based methods estimate chl-*a* concentration indirectly via emitted light from excited pigments; however, fluorescence yield varies with physiological state, species composition, pigment packaging, and environmental conditions (Roesler *et al.*, 2017; Hodges *et al.*, 2018). Consequently, a linear and uniform relationship between fluorescence and extracted chl-*a* is rarely achieved in heterogeneous natural systems. Furthermore, this global relationship is primarily driven by high-biomass observations, rather than representing a consistent performance across the full concentration range.

The complete breakdown of the relationship below 10 μg L^{-1} is particularly informative. At low biomass, fluorescence signals approach the instrument's detection

threshold, and background optical noise (e.g., coloured dissolved organic matter (CDOM), suspended particles, carbon from plant sources) may dominate the signal, distorting readings (Le & Wilson, 2025). In such conditions, small differences in pigment concentration produce negligible changes in fluorescence output, explaining the near-zero explanatory power in the low-concentration subset (R^2 = 0.0001, Table 4). This phenomenon has been documented in other freshwater systems, where fluorometric accuracy declines sharply under oligotrophic or mesotrophic conditions (Thomson-Laing *et al.,* 2020; Hamdhani *et al.,* 2021).

In contrast, improved correspondence under bloom conditions indicates that fluorescence becomes more reliable when pigment concentrations exceed background variability. However, even at higher biomass, explanatory power remained weak (R^2 = 0.18, Table 4), suggesting additional sources of variability, such as differences in other dissolved compounds like organic matter or geothermal solutes at different sites.

Negative outliers observed at high laboratory chl-*a* values are consistent with bloom senescence, in which pigment degradation or an altered physiological state reduces emitted fluorescence. Conversely, positive outliers may reflect actively growing phytoplankton with high photosynthetic efficiency, resulting in disproportionately strong fluorescence relative to extracted chl-*a*. Conclusively, outliers that persist across the same weeks and sites likely reflect real ecological complexity rather than simple sensor error. Rapid bloom formation, patchiness, vertical water-column structure, mixing, and variable pigment composition all complicate the translation of fluorescence signals into biomass estimates.

Spatial heterogeneity in sensor performance also suggests variation in phytoplankton community composition. Cyanobacteria, which frequently dominate blooms in Lake Rotorua, contain accessory pigments (e.g., phycocyanin) that may influence fluorescence signatures and spectral overlap (Codd *et al.*, 2005). Future analyses, which measure phycocyanin using

laboratory extraction, should be conducted to better understand the spatial variability of cyanobacteria specifically. Additionally, geothermal inputs characteristic of Lake Rotorua introduce dissolved solutes (e.g., silica, sulphur, chloride) that may modify optical properties (i.e., water colour) and interfere with fluorescence detection (Donovan & Donovan, 2003; Pearson *et al.,* 2010; Wu *et al.,* 2023).

The strong site-specific regressions observed at Te Pōhue and Hamurana (West) indicate that under relatively consistent optical and ecological conditions, fluorescence can provide a robust proxy for extracted chl-*a*. However, the variability observed elsewhere underscores the need for local calibration. Fluorometric relationships are context-dependent and should be interpreted within the optical and ecological characteristics of each monitoring site (Cotterill *et al.,* 2019).

Integrated Implications for Monitoring and Forecasting using the Hand-held FluoroQuik

Together, these results demonstrate that Lake Rotorua's nearshore bloom regime is dynamic, disturbance-driven, and spatially compartmentalised. Episodic nutrient mobilisation, wind redistribution, and inflow-associated enrichment generate rapid and spatially heterogeneous biomass fluctuations that cannot be resolved through low-frequency or single-site monitoring.

Within this context, hand-held fluorescence sensing provides clear operational value for early warning, bloom surveillance, and rapid assessment under high-biomass conditions. However, its reduced sensitivity at low biomass and site-specific variability limit its suitability for regulatory-grade concentration estimation, compliance monitoring, or threshold enforcement. Consequently, reliance on uncalibrated sensor data may risk misinterpretation of ecological conditions.

The most effective application of the FluoroQuik lies within hybrid monitoring frameworks that combine high-frequency fluorometric screening with periodic laboratory validation and site-specific calibration. Integration with hydrodynamic and meteorological forecasting tools (e.g., LakeCast) could further enhance detection of bloom onset and short-term trend dynamics by improving temporal resolution. However, sensor-derived data should not be used for absolute concentration forecasting or regulatory threshold modelling without laboratory support.

In eutrophic polymictic systems–such as Lake Rotorua–susceptible to legacy nutrient pressures and climatic variability, monitoring strategies must align with the temporal and spatial scale of bloom drivers. The patterns documented here reinforce the need for adaptive, spatially resolved, and mechanistically informed monitoring approaches to effectively manage ecological and public health risks.

Limitations

Several limitations should be considered when interpreting these findings. Spatial coverage was restricted to nine nearshore sites, which does not include a fully resolved spatial representation of Lake Rotorua's shoreline variability. One additional lakefront site was excluded due to interference from seaweed extraction and human disturbance early in the study, further constraining spatial completeness. While the selected sites captured key inflow- and wind-influenced zones, broader lakefront coverage would improve spatial generalisability. Sampling intensity was also limited. Only a single replicate was collected per site per week due to laboratory processing constraints, reducing the ability to quantify within-site variability. Following weekly averaging of the duplicates from the first week, the effective sample size was modest (n = 54; 9 sites*6 weeks), which likely reduced statistical power and contributed to moderate R^2 values in regression analyses. Future studies incorporating greater replication

and extended sampling duration would strengthen inference and improve calibration robustness. Additional methodological uncertainty may have arisen from manual handling procedures, including pipetting accuracy, dilution selection, filtration consistency, storage conditions, and general sample handling. Water collection relied on a single bucket per site, from which a single syringe subsample (20–30 mL) was extracted, potentially limiting representation of small-scale heterogeneity within the water column. Although standardised protocols were followed, these steps introduced cumulative sources of variability inherent in field–laboratory workflows. Temporal coverage was interrupted by a two-week gap in late December to early January (22 December 2025 – 4 January 2026), preventing resolution of bloom dynamics during this period. Given the disturbance-driven and episodic nature of nearshore blooms, unobserved short-term events may have occurred. Finally, while chl-*a* is widely used as a proxy for algal biomass, it does not directly distinguish cyanobacterial dominance or toxin risk. Phycocyanin has been shown to exhibit strong relationships with cyanobacterial biovolume (e.g., Hodges *et al.*, 2018; Cotterill *et al.*, 2019; Thomson-Laing et al., 2020) and may provide a more targeted indicator of bloom toxicity. Future comparisons between handheld fluorometric sensors and laboratory analyses would benefit from incorporating phycocyanin measurements to better evaluate cyanobacteria-specific dynamics.

Acknowledgements: This research was conducted as part of the LakeCast project, MBIE Grant UOWX2434. I thank Whitney Woelmer, Deniz Özkundakci, and Amohia Peka for their guidance and support throughout the project. I acknowledge Te Arawa Lakes Trust and the University of Waikato (School of Science) for institutional support and collaboration. Thanks go to Chloe Kayll-Irvine and Kat Rowe for laboratory and field assistance. We also acknowledge all partners involved in LakeCast for their contributions toward improving algal bloom monitoring and forecasting in Lake Rotorua. Thank you to the Summer Research Scholarship 2025 Programme for this opportunity.

References

Britton, L. J., Averett, R. C., & Ferreira, R. F. (1975). *An introduction to the processes, problems, and management of urban lakes*. Circular 601-K. US Department of the Interior, Geological Survey. https://doi.org/10.3133/cir601K

Burns, C. W. (1991). New Zealand lakes research, 1967–91. *New Zealand Journal of Marine and Freshwater Research, 25* (4), 359-379. https://doi.org/10.1080/00288330.1991.9516491

Burns, N., McIntosh, J., & Scholes, P. (2005). Strategies for managing the lakes of the Rotorua District, New Zealand. *Lake and reservoir management, 21* (1), 61-72. https://doi.org/10.1080/07438140509354413

Burns, N. M., Rutherford, J. C., & Clayton, J. S. (1999). A monitoring and classification system for New Zealand lakes and reservoirs. *Lake and reservoir management, 15* (4), 255-271. https://doi.org/10.1080/07438149909354122

Codd, G. A., Morrison, L. F., & Metcalf, J. S. (2005). Cyanobacterial toxins: risk management for health protection. *Toxicology and Applied Pharmacology, 203* (3), 264-272. https://doi.org/10.1016/j.taap.2004.02.016

Cotterill, V., Hamilton, D. P., Puddick, J., Suren, A., & Wood, S. A. (2019). Phycocyanin sensors as an early warning system for cyanobacteria blooms concentrations: a case study in the Rotorua lakes. *New Zealand Journal of Marine and Freshwater Research, 53* (4), 555-570. https://doi.org/10.1080/00288330.2019.1617322

Deng, J., Qin, B., Sarvala, J., Salmaso, N., Zhu, G., Ventelä, A. M., ... & Vuorio, K. (2016). Phytoplankton assemblages respond differently to climate warming and eutrophication: A case study from Pyhäjärvi and Taihu. *Journal of Great Lakes Research, 42* (2), 386-396. https://doi.org/10.1016/j.jglr.2015.12.008

Donovan, C. L., & Donovan, W. F. (2003). *Estimate of the Geothermal Nutrient Inputs to Twelve Rotorua Lakes*. Bioresearches, Consulting Biologists & Archaeologists. https://atlas.boprc.govt.nz/api/v1/edms/document/A685171/content

Hamdhani, H., Eppehimer, D. E., Walker, D., & Bogan, M. T. (2021). Performance of a handheld chlorophyll-a fluorometer: Potential use for rapid algae monitoring. *Water, 13* (10), 1409. https://doi.org/10.3390/w13101409

Hamilton, D. P. (2003). A historical and contemporary review of water quality in the Rotorua lakes. *Rotorua Lakes Proceedings*, pp. 3-15. https://lakeswaterquality.co.nz/wp-content/uploads/symposiums/2003-Symposium-proceddings.pdf

Ho, J. C., Michalak, A. M., & Pahlevan, N. (2019). Widespread global increase in intense lake phytoplankton blooms since the 1980s. *Nature, 574* (7780), 667-670. https://doi.org/10.1038/s41586-019-1648-7

Hodges, C. M., Wood, S. A., Puddick, J., McBride, C. G., & Hamilton, D. P. (2018). Sensor manufacturer, temperature, and cyanobacteria morphology affect phycocyanin fluorescence measurements. *Environmental Science and Pollution Research, 25* (2), 1079-1088. https://doi.org/10.1007/s11356-017-0473-5

Hötzel, G., & Croome, R. (1999). A phytoplankton methods manual for Australian freshwaters. *LWRRDC Occasional Paper 22/99.* Land and Water Research and Development Corporation: Canberra. https://library.dbca.wa.gov.au/static/Journals/082185/082185-1999.22.pdf

Kraft, K., Haraguchi, L., Hällfors, H., Suikkanen, S., Ylöstalo, P., Kielosto, S., ... & Seppälä, J. (2025). Monitoring cyanobacteria blooms with complementary measurements–a similar story told using high-throughput imaging, optical sensors, light microscopy, and satellite-based methods. *Harmful Algae*, 102865. https://doi.org/10.1016/j.hal.2025.102865

Le, V. V., & Wilson, A. E. (2025). A handheld fluorometer evaluates freshwater cyanobacterial blooms across a broad productivity gradient. *Lake and Reservoir Management, 41* (2), 104-111. https://doi.org/10.1080/10402381.2025.2484690

McColl, R. H. S. (1972). Chemistry and trophic status of seven New Zealand lakes. *New Zealand Journal of Marine and Freshwater Research, 6* (4), 399-447.

Ministry for the Environment. (2025). *National Policy Statement for Freshwater Management 2020 (as amended December 2025)*. https://environment.govt.nz/acts-and-regulations/national-policy-statements/national-policy-statement-freshwater-management/

Moss, B. (1998). *Ecology of Freshwaters: Man and medium, past to future*. 3rd Edition. Blackwell Science, Oxford/Malden MA. 557pp.

Mueller, H., Hamilton, D. P., & Doole, G. J. (2015). Response lags and environmental dynamics of restoration efforts for Lake Rotorua, New Zealand. *Environmental Research Letters, 10* (7), 074003. https://doi.org/10.1088/1748-9326/10/7/074003

Müller, K., & Wickham, H. (2026). *tibble: Simple Data Frames* (R package version 3.3.1) [Computer software]. https://tibble.tidyverse.org/

Nelson, N., Sander, D., Dandin, M., Prakash, S. B., Sarje, A., & Abshire, P. (2009). Handheld fluorometers for lab-on-a-chip applications. *IEEE Transactions on Biomedical Circuits and Systems, 3* (2), 97-107. https://doi.org/10.1109/TBCAS.2008.2006494

O'Neil, J. M., Davis, T. W., Burford, M. A., & Gobler, C. J. (2012). The rise of harmful cyanobacteria blooms: the potential roles of eutrophication and climate change. *Harmful algae, 14*, 313-334. https://doi.org/10.1016/j.hal.2011.10.027

Paerl, H. W., Otten, T. G., & Kudela, R. (2018). Mitigating the expansion of harmful algal blooms across the freshwater-to-marine continuum. *Environmental Science & Technology*, 52(10), 5519-5529. https://doi.org/10.1021/acs.est.7b05950

Pearson, L. K., Hendy, C. H., Hamilton, D. P., & Pickett, R. C. (2010). Natural and anthropogenic lead in sediments of the Rotorua lakes, New Zealand. *Earth and Planetary Science Letters, 297* (3-4), 536-544. https://doi.org/10.1016/j.epsl.2010.07.005

Pedersen, T. L. (2025). *patchwork: The Composer of Plots* (R package version 1.3.2.9000). https://patchwork.data-imaginist.com/

R Core Team. (2022). R: A language and environment for statistical computing (Version 4.2.2) [Computer software]. R Foundation for Statistical Computing. https://www.R-project.org/

Reynolds, C. S., Huszar, V., Kruk, C., Naselli-Flores, L., & Melo, S. (2002). Towards a functional classification of the freshwater phytoplankton. *Journal of Plankton Research, 24* (5), 417-428. https://doi.org/10.1093/plankt/24.5.417

Roesler, C., Uitz, J., Claustre, H., Boss, E., Xing, X., Organelli, E., ... & Barbieux, M. (2017). Recommendations for obtaining unbiased chlorophyll estimates from in situ chlorophyll fluorometers: A global analysis of WET Labs ECO sensors. *Limnology and Oceanography: Methods, 15* (6), 572-585. https://doi.org/10.1002/lom3.10185

RStudio Team. (2022). RStudio: Integrated development environment for R [Computer software]. RStudio, PBC. https://posit.co/

Rutherford, J. C., Dumnov, S. M. & Ross, A. H. (1996). Predictions of phosphorus in Lake Rotorua following load reductions. *New Zealand Journal of Marine and Freshwater Research*, 30: 383-396. https://doi.org/10.1080/00288330.1996.9516725

Thomson-Laing, G., Puddick, J., & Wood, S. A. (2020). Predicting cyanobacterial biovolumes from phycocyanin fluorescence using a handheld fluorometer in the field. *Harmful Algae, 97*, 101869. https://doi.org/10.1016/j.hal.2020.101869

Time and Date AS [1995-2026]. (2026). *Past weather in Rotorua, New Zealand — Historic weather*. https://www.timeanddate.com/weather/new-zealand/rotorua/historic

Wickham, H. (2016). Data analysis. In: ggplot2: elegant graphics for data analysis (pp. 189-201). Cham: Springer International Publishing.

Wickham, H., François, R., Henry, L., Müller, K., Vaughan, D. (2025). dplyr: A Grammar of Data Manipulation. R package version 1.1.4, https://dplyr.tidyverse.org

Wilke, C. O. (2025). *cowplot: Streamlined Plot Theme and Plot Annotations for 'ggplot2'* (R package version 1.2.0). https://link.springer.com/book/10.1007/978-3-319-24277-4#toc

Wu, N., Guo, K., Suren, A. M., & Riis, T. (2023). Lake morphological characteristics and climatic factors affect long-term trends of phytoplankton community in the Rotorua Te Arawa lakes, New Zealand during 23 years observation. *Water Research, 229*, 119469. https://doi.org/10.1016/j.watres.2022.119469